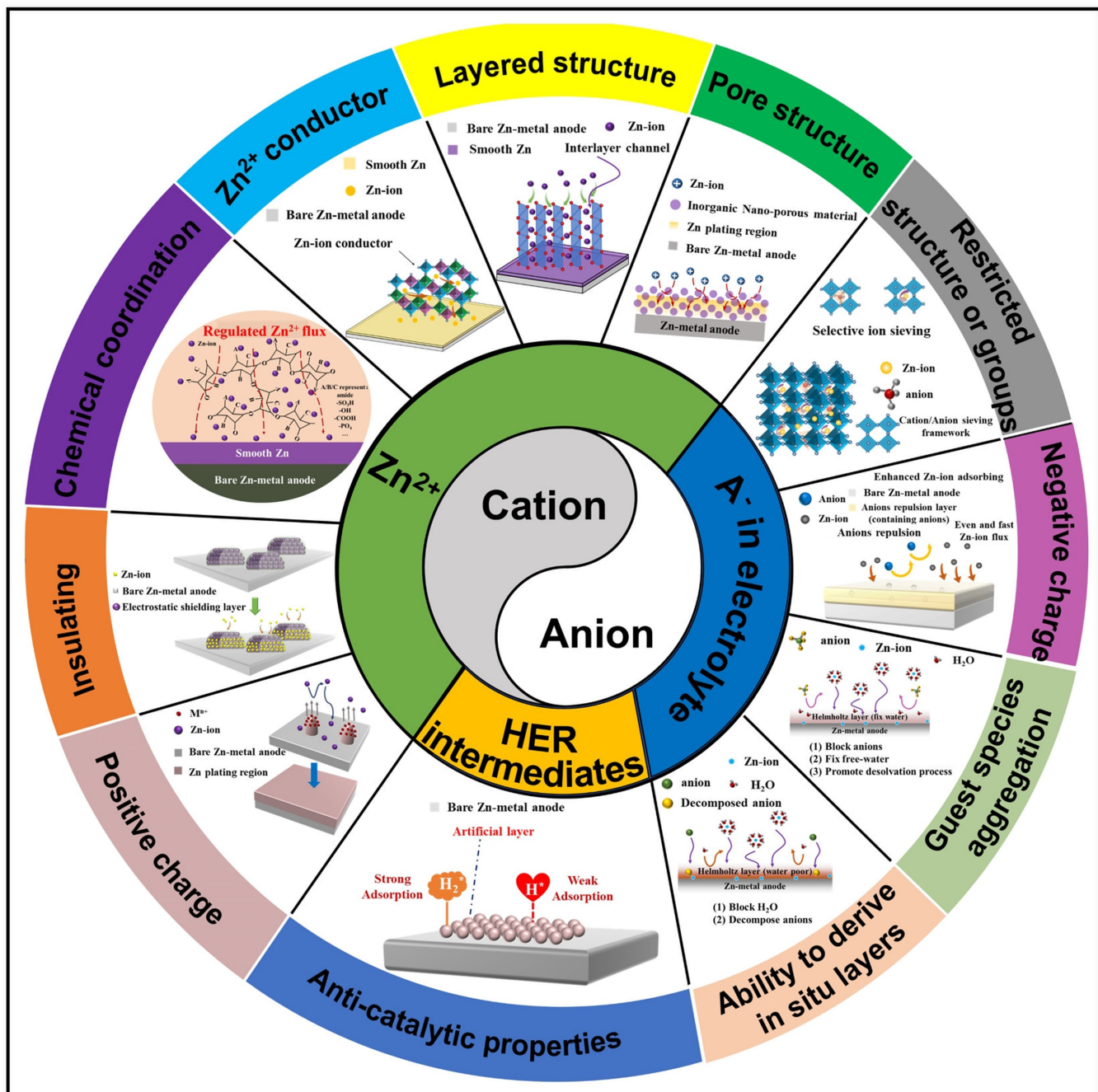


Cation and Anion Modulation Strategies toward Ideal Zinc Artificial Interface

Jingjing Yang^{+[a]}, Anqi Zhang^{+[a]}, Ran Zhao,^{*[a]} Chuan Wu,^{*[a, b]} and Ying Bai^{*[a]}



Aqueous zinc-ion batteries (ZIBs) stand out as promising next-generation energy storage systems. However, the Zn anode failure caused by the unstable Zn/electrolyte interface hinders their practical applications. Constructing artificial layer on the Zn surface provides an effective method to optimize the interfacial stability and mitigate the issues, while most of the current investigations put emphasis on the discussion of Zn^{2+} and H_2O regulation, we notice that the anions and hydrogen evolution reaction (HER) intermediates also play a crucial role in the occurrence of side reactions, thus a comprehensive evaluation of interfacial modulation strategies regarding all the

different ion species in ZIBs system is helpful for developing advanced artificial interface. Herein, this work systematically reviews the achievements about cation and anion modulation strategies for stabilizing Zn/electrolyte interface and emphasizes on the relationship between the material properties and ionic regulation mechanisms for the first time, aiming to provide an unprecedented design reference. Furthermore, some noteworthy points and perspectives are proposed, which has guiding significance for the realization of high-performance and multi-level regulated Zn anode.

1. Introduction

Highly developed societies and dramatically increasing energy demands have stimulated the development of low-cost and high-performance energy storage and conversion devices.^[1] With the advantages of inherent safety, high ionic conductivity, low manufacturing cost, and superior sustainability, rechargeable aqueous zinc-ion batteries (ZIBs) emerge as a promising next-generation battery technology, especially in the field of large-scale energy storage.^[2] Based on the two-electron reaction and appropriate overpotential, the direct application of Zn metal anodes leads to competitive performance, exhibiting high capacities of 820 mAhg^{-1} and 5855 mAh cm^{-3} .^[3] However, the further development of ZIBs is hindered by Zn anode failures. The formation of Zn dendrites and the occurrence of the undesirable side reactions, involving hydrogen evolution reaction (HER), corrosion and passivation, resulting in short circuit with limited lifespan and poor reversibility with low Coulombic efficiency (CE).^[4] Therefore, there is an urgent need to design and develop a stable Zn/electrolyte artificial interface to alleviate the above affection and maximize the inherent advantages of ZIBs based on Zn metal anodes.

Tremendous attempts and efforts have been made to overcome the problems of Zn anode and numerous reviews have provided guidance for stabilizing Zn anode. However, most reviews put emphasis on one or more specific modification methods, such as Zn structure design, alloying strategy, surface modification, electrolyte optimization, and separator design.^[5] Focusing on a specific modification approach leads to the ignorance of the structure-activity relationship between intrinsic properties and protection performance, resulting in

limitations for the further performance improvement. Notably, optimizing the Zn/electrolyte interface has been proven to be an effective method, and the construction of artificial layers on Zn surfaces has attracted extensive attention due to its high efficiency and potential for large-scale fabrication and commercialization.^[6] Previous reviews regarding Zn artificial interphase generally pay attention to different protection materials or certain protection mechanisms.^[7] For example, the application of carbon materials,^[8] and metal-organic frameworks (MOFs) materials^[7a] in improving the Zn metal anode in AZIBs have been comprehensively reviewed and discussed. In addition, Li et al.^[7c] discussed the protection mechanism about horizontally oriented Zn anode for uniform Zn deposition and analyzed the crucial factors in detail. The correlation between different modification materials and the regulation of cation and anion in the battery system is usually ignored, leaving room for a detailed discussion on the strategies in terms of the ionic flux regulations.

The formation and growth of Zn dendrites usually involve the inhomogeneous distribution of electric field and Zn^{2+} flux, and the side reactions occurring on the Zn surface are highly related to active water molecules.^[6a,g] Therefore, most of the current studies put emphasis on the discussion of Zn^{2+} and H_2O regulation. However, the crucial roles of anions and HER intermediates (H_3O^+ species and H^*) directly participating in the formation of $Zn_4SO_4(OH)_6 \cdot xH_2O$ (ZHS) by-products and the HER process have been rarely received attention. In addition, we also notice that the reconstructed electric double layer (EDL) and derivatized layer on the Zn surface can be achieved via species regulation in the electrolyte. Therefore, a comprehensive evaluation of the regulation methods of these ions is helpful for the construction of advanced Zn artificial layers.

Herein, according to the essential regulation principles, achievements regarding cation and anion modulation strategies for stabilizing Zn/electrolyte interface are systematically reviewed. In addition, this review uniquely emphasizes and analyzes the relationship between the material properties and cation/anion regulation functions for the first time, including the regulation of Zn^{2+} flux, HER intermediates (H_3O^+ and H^*) and anions in the electrolytes, aiming to provide an unprecedented design reference to develop high-performance and multi-level regulated Zn anodes. In particular, the modulation of Zn^{2+} flux based on lattice transport and chemical coordination, as well as some anion modulation strategies that are rarely

[a] Dr. J. Yang,[†] Dr. A. Zhang,[†] Dr. R. Zhao, Prof. C. Wu, Prof. Y. Bai
Department Beijing Key Laboratory of Environmental Science and Engineering
School of Materials Science and Engineering
Beijing Institute of Technology, Beijing 100081, PR China
E-mail: 7520210029@bit.edu.cn
chuanwu@bit.edu.cn
membrane@bit.edu.cn

[b] Prof. C. Wu
Yangtze Delta Region Academy of Beijing Institute of Technology
Jiaxing 314019, PR China
E-mail: chuanwu@bit.edu.cn

[†] These authors contributed equally to this work.

mentioned in previously reported reviews are discussed in detail. Finally, noteworthy points and perspectives for further development toward stable Zn/electrolyte interfaces are also proposed.

2. Zn²⁺ Flux Modulation Strategies

The Zn²⁺ flux modulation strategy has a significant effect on guiding uniform Zn deposition. At present, many Zn²⁺ flux modulation strategies have been proposed, including introducing pore structure, layered structure and Zn²⁺ conductor layers on Zn anodes, as well as the optimization strategies by the interaction of chemical coordination, insulating, and positive charge repulsion effect.

2.1. Pore structure

The homogeneous pore structure has a high specific surface area, providing sufficient zincophilic sites, short and open ion diffusion channels, more uniform electric field and concentration field, which is expected to accelerate the diffusion of Zn²⁺ and limit the occurrence of competitive side reactions. At present, pore structure engineering as a strategy to regulate Zn²⁺ flux mainly focuses on the construction of two-dimen-

sional (2D) nanopores^[10] and three-dimensional (3D) frameworks.

2.1.1. Nanopore

The coating of porous polymer-BaTiO₃ (BTO) can significantly uniformize the Zn²⁺ distribution and accelerate the Zn²⁺ diffusion at the interface through homo-channeling effect, thereby inhibiting the formation of Zn dendrites (Figure 1a).^[11] In addition, a dense Zn plating layer formed between CaCO₃ coating layer and Zn foil leads to a sandwich structure of "CaCO₃/Zn plating/Zn foil", bringing about the occurrence of Zn²⁺ reduction only when the potential is negative enough (Figure 1b).^[12] Besides, 2D mesoporous zincophilic sieve (2DZS) was also applied as a protective materials.^[13]

In general, the coating of porous structure on Zn anode surface can provide nano-channel for ion transport and regulate the distribution of Zn²⁺ flow to avoid the growth of Zn dendrites, and promote the cycling stability of LIBs.

2.1.2. Framework

As shown in Figure 1c, the prepared polyanionic hydrogel film (Zn-SHn) with a strong hydrogel-solid adhesion can significantly



Jingjing Yang received her bachelor's degree from Beijing University of Technology (BJUT) in 2020. She is currently a Ph.D. candidate supervised by Prof. Chuan Wu in School of Materials Science and Engineering, Beijing Institute of Technology (BIT). Her research interests focus on the design of high-performance electrolytes and electrode materials for aqueous zinc-ion batteries.



Anqi Zhang received her master's degree from Beijing University of Chemical Technology (BUCT) in 2021. She is currently a Ph.D. candidate supervised by Prof. Ying Bai in School of Materials Science and Engineering, Beijing Institute of Technology (BIT). Her research interests focus on the design of high-performance electrode materials for aqueous zinc-ion batteries.



Ran Zhao currently works as a post-doctoral fellow at Beijing Institute of Technology (BIT). She received her Ph.D. degree in Chemistry from Arizona State University in 2017 and worked as a research associate in Iowa State University from 2017 to 2019, followed by a one-year research experience in Arizona State University. Her main research interests are key materials for secondary multivalent ion batteries and sulfide-based solid-state electrolytes.



Ying Bai is currently a professor at Beijing Institute of Technology (BIT). Her research interests focus on electrochemical energy storage and conversion technology. She completed her Ph.D. from School of Chemical Engineering & Materials Science at BIT in 2003. In 2013, she was awarded New Century Excellent Talents in University from the Chinese Ministry of Education. She hosted and is hosting the projects of the National Natural Science Foundation of China as a principal investigator.



Chuan Wu is a professor at Beijing Institute of Technology (BIT), where his interests are new energy materials, and secondary batteries based on multi-electron materials. He received his Ph.D. degree in Applied Chemistry from BIT in 2002, followed by a 2-year postdoctoral fellowship in Dalian Institute of Chemical Physics, Chinese Academy of Sciences. Dr. Wu was awarded Beijing Outstanding Talents Cultivation Project in 2007, Beijing Nova Program Award in 2009, and New Century Excellent Talents in University in 2012.

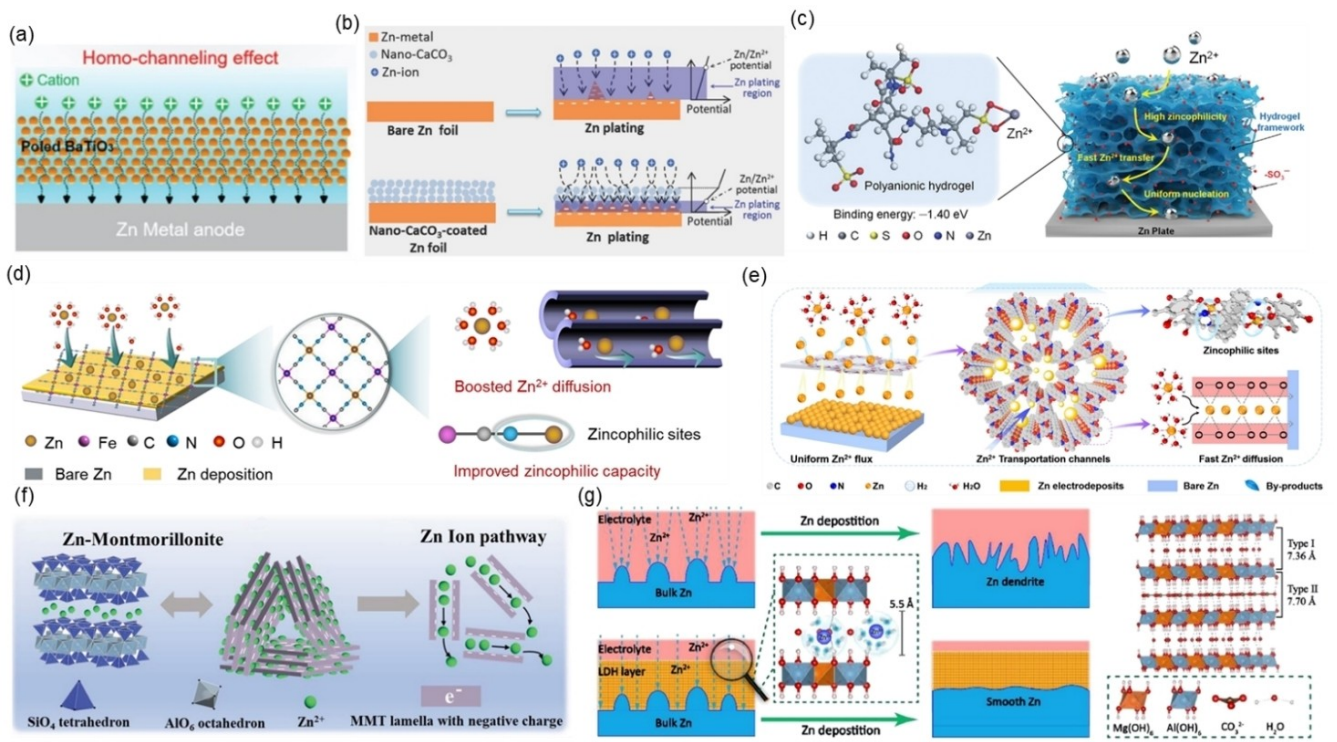


Figure 1. a) Schematic diagram of Zn²⁺ diffusion in nano-porous polymer-BTO coatings. Reproduced with permission from Ref. [11]. Copyright (2021) Wiley-VCH. b) Schematic diagram of Zn plating on nano-CaCO₃-coated Zn foils and bare Zn. Reproduced with permission from Ref. [13]. Copyright (2018) Wiley-VCH. c) Schematic diagram of Zn²⁺ diffusion in polyanionic hydrogel layer. Reproduced with permission from Ref. [14]. Copyright (2022) Wiley-VCH. Schematic diagram of Zn plating on d) MOF@Zn electrode, and e) Zn-COF@Zn surface. Reproduced with permission from Refs. [15] and [16]. Copyright (2023) American Chemical Society. Copyright (2022) Wiley-VCH. f) Schematic diagram of Zn²⁺ diffusion in MMT-Zn. Reproduced with permission from Ref. [22]. Copyright (2021) Wiley-VCH. g) Schematic diagram of Zn plating on bare Zn and Zn@LDH electrode. Reproduced with permission from Ref. [23]. Copyright (2021) Elsevier B.V.

regulate the Zn²⁺ flux via framework.^[14] With a 3D open frame in Figure 1d, the metal-organic framework (MOF) modified layer can not only facilitate the desolvation process, but also provide ordered nanochannels to achieve homogeneous Zn²⁺ flux and inhibit the side reaction.^[15] Similar with MOF, the covalent organic frameworks (COFs) could also effectively regulate the solvation structure, as well as the Zn²⁺ flux (Figure 1e).^[16]

The construction of 3D frameworks can effectively homogenize the distribution of Zn²⁺ flux, optimize the nucleation process, and inhibit or delay the growth of Zn dendrites. Currently, research on 3D framework construction with regulatory effect on Zn²⁺ flux mainly concentrate on MOF,^[17] COF,^[18] ball milling clay precipitate (designated as BMC, consisting of the unetched MAX phase and the Ti₃C₂T_x phase)^[19] and intriguing ion sieve,^[20] etc.

2.2. Layered structure

Inspired by the construction of solid electrolyte interface (SEI) in lithium-ion batteries (LIBs), artificial interface layer with abundant ion channels are selected to protect Zn anode, which can effectively uniform Zn²⁺ flux distribution for stable and rapid Zn plating/stripping.^[21]

Zn-based montmorillonite (Zn-MMT) is a layered silicate lamellar with negative electric properties, which not only has good Zn²⁺ attraction properties, but also has high-speed channels for transmitting Zn²⁺ (Figure 1f).^[22] In Figure 1g, by constructing Mg-Al layered double hydroxide (LDH) on the Zn anode, suitable interlayer channel is provided to redistribute Zn²⁺ flux and accelerate the transport of Zn²⁺ ions.^[23]

Therefore, the constructed coatings with layered structure deliver an effective strategy to inhibit Zn dendrites and improve the stability of ZIBs.

2.3. Zn²⁺ conductor

Notably, due to the inherent ion conductive property, the fast Zn²⁺ conductor has been paid enough attention in the development of the ASEI.^[24] In recent, ZnO HF conductor^[25] (Figure 2a) and NaTi₂(PO₄)₃ (NTP) consisting of TiO₆ octahedra and PO₄ tetrahedra^[24] with weak electron conductivity and fast Zn²⁺ conductivity have been proposed. In Figure 2b, Zn²⁺ can be transported rapidly in the remaining void composed of oxygen atoms with a low migration barrier, resulting in a faster Zn transportation kinetics on Zn anode.

The artificial layer with high Zn²⁺ transport kinetics as an ion passable fence can regulate ion transport, uniform Zn²⁺

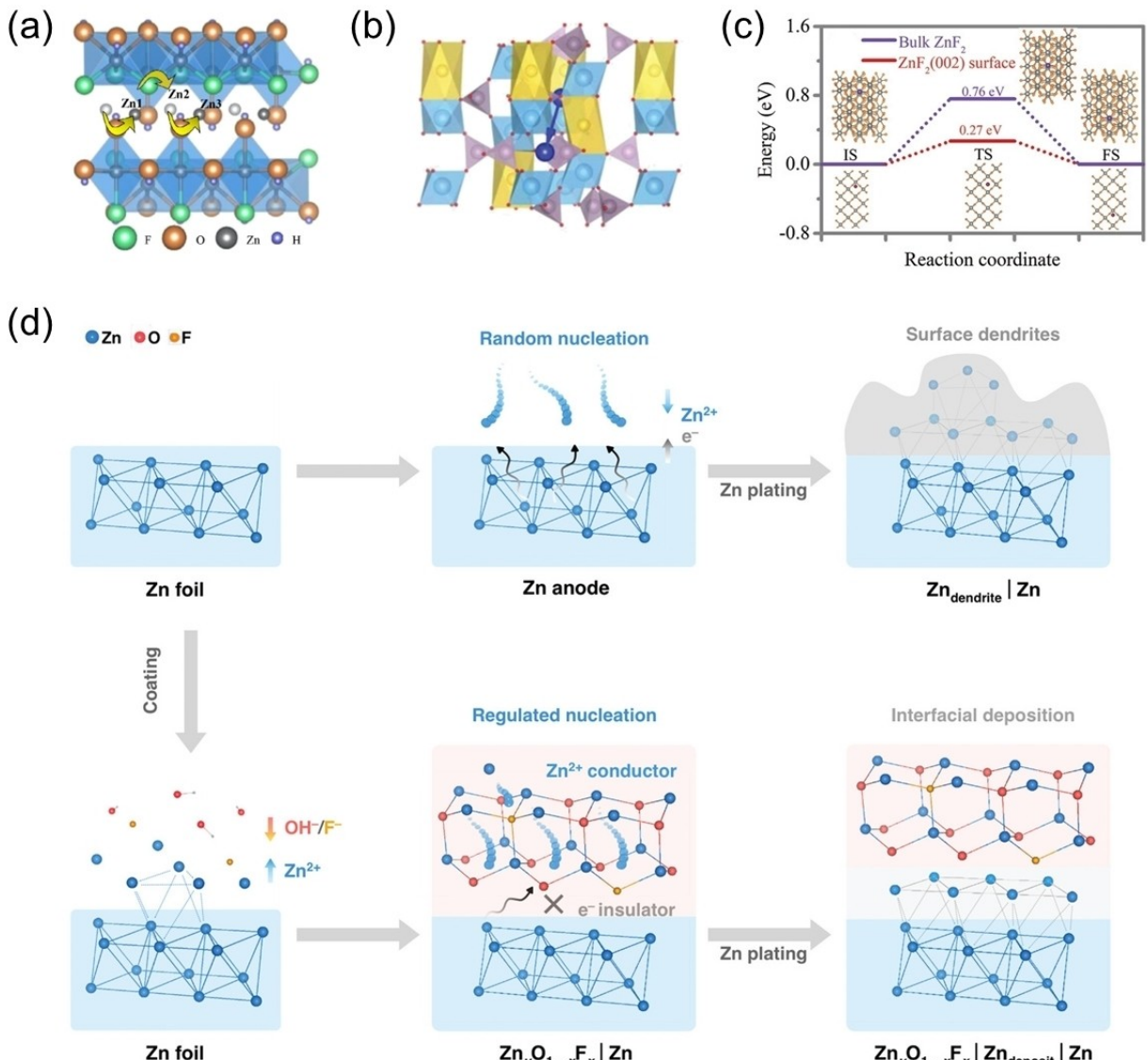


Figure 2. Schematic diagram of Zn ion migration path in a) ZnOHF and b) NTP layer. Reproduced with permission from Ref. [25]. Copyright (2023) Elsevier Ltd. Reproduced with permission from Ref. [24]. Copyright (2020) Wiley-VCH. c) Schematic diagram of the migration energy barrier of Zn²⁺ on ZnF₂(002) surface and in ZnF₂. Reproduced with permission from Ref. [26]. Copyright (2021) Wiley-VCH. d) Zinc ion conduction of zinc oxide fluoride protective layer. Reproduced with permission from Ref. [27]. Copyright (2023) Wiley-VCH.

flux, optimize Zn deposition behavior, and significantly inhibit dendrite growth. Besides the ZnOHF and NTP, ZnF₂^[26] (Figure 2c) and zinc oxide fluoride^[27] (Figure 2d) were also proven to be fast conductors for Zn²⁺ transport, thus realizing homogenized Zn deposition.

2.4. Chemical coordination

Recently, developing artificial interface layer with strong coordination with Zn²⁺ has aroused attention. Due to the coordination interaction with Zn²⁺, the ASEI affects the Zn²⁺ distribution and diffusion behavior,^[28] which can optimize the Zn stripping/plating behavior^[10] and improve the electrochemical polarization and nucleation overpotentials.^[29] Specifically,

the artificial layer modification would change the nucleation barrier on the Zn surface, which is highly related to electrical field, ion concentration and surface energy, thus affecting the nucleation overpotential.^[30] In addition, the constructed coating may impede the access of Zn²⁺ to the Zn surface, resulting in constrained kinetic and large overpotentials.^[31] Therefore, the built organic coatings exhibited different overpotential (Table 1).

The organic materials usually coordinate Zn²⁺ through zincophilic sites. Phytic acid (PA) molecule with six phosphate groups can form stable Zn-PA cross-linked network with Zn²⁺ (Figure 3a), thereby decreasing the transmission barrier of Zn²⁺ to inhibit Zn dendrite and reduce polarization.^[32] In addition, Zn-alginate (Alg) network with core-shell structure (Figure 3b)^[33] and zincophilic molecular brushes (Figure 3c)^[34] can also

Table 1. Summary of the effects of anion/cation modulation strategies, including coating materials, protection mechanisms, and cell performance.

Modulation strategies	Artificial interphase materials	Material properties	Electrolyte	Cyclic performance	CE	Refs.
Zn ²⁺ flux	Nano-porous BaTiO ₃	Nanopore	1 M ZnSO ₄ + 0.1 M MnSO ₄	Over 4100 h at 1 mA cm ⁻² with voltage hysteresis of between ≈30–50 mV	Above 99% over 1000 cycles at 3 mA cm ⁻²	[11]
Zn ²⁺ flux	Porous nano-CaCO ₃	Nanopore	3 M ZnSO ₄ + 0.1 M MnSO ₄	Over 836 h at 0.25 mA cm ⁻² with polarization ≈105 mV	84.7% within 1000 cycles at 1 A g ⁻¹	[12]
Zn ²⁺ flux	Two-dimensional mesoporous ZnS	Nanopore	2 M ZnSO ₄	Over 900 h at 2 mA cm ⁻² with polarization ≈26 mV / at 20 mA cm ⁻² with polarization ≈48 mV / at 80 mA cm ⁻² with polarization ≈130 mV	98.9% within 1200 cycles at 2 mA cm ⁻²	[13]
Zn ²⁺ flux	A polyanionic hydrogel film with negatively charge (−SO ₃ [−])	Framework	2 M ZnSO ₄	Over 3500 h at 1 mA cm ⁻² with polarization voltage around 50 mV	Around 99% after 150 cycles under 1 mA cm ⁻² / 1 mA h cm ⁻²	[14]
Zn ²⁺ flux	Metal-organic frameworks (MOFs) with 3D open framework	Framework	2 M ZnSO ₄	Over 1100 h at 10 mA cm ⁻² with polarization voltages of 67 mV	99.2% over 1000 cycles and prolonged lifetime of 1100 h at 10 mA cm ⁻²	[15]
Zn ²⁺ flux	Zincophilic metal-covalent organic frameworks (COFs) (Zn-AAm-COF)	Framework	1 M ZnSO ₄	Over 3000 cycles at 20 mA cm ⁻² with overpotential ≈79.1 mV	99.3% after 100 cycles at 20 mA cm ⁻²	[16]
Zn ²⁺ flux	3D ZnO/C nanoparticles (3D-ZGC) framework	Framework	1 M ZnSO ₄	150 h at 20 mA cm ⁻² with Overpotential < 65 mV	99.4% after 300 cycles at 20 mA cm ⁻²	[17]
Zn ²⁺ flux	layered kaolin with uniform-pore distribution	Layered structure	2 M ZnSO ₄ + 0.1 M MnSO ₄	Over 800 h at 4.4 mA cm ⁻² with voltage hysteresis of 70 mV	—	[21]
Zn ²⁺ flux	Layered Zn-based montmorillonite (MMT)	Layered structure	2 M ZnSO ₄	Over 1,000 h at 10 mA cm ⁻² /45 mAh cm ⁻² with overpotential ≈100 mV	96.3% after 50 h at 1 mA cm ⁻²	[22]
Zn ²⁺ flux	Mg-Al layered double hydroxide (LDH)	Layered structure	2 M ZnSO ₄	Over 1400 h at 0.5 mA cm ⁻² with voltage polarization ≈31.6 mV	99.2% for a lifespan of 1400 h at 0.5 mA cm ⁻²	[23]
Zn ²⁺ flux	NaTi ₂ (PO ₄) ₃ (NTP) ion conductor	Zn ²⁺ conductor	2 M ZnSO ₄ + 0.2 M MnSO ₄	During 80 h at 1 mA cm ⁻² with polarization voltage ≈30–50 mV	Nearly 100% after 10 000 charge/discharge cycles at 10 C (≈1.5 A g ⁻¹)	[24]
Zn ²⁺ flux	ZnOHF conductor film	Zn ²⁺ conductor	2 M ZnSO ₄	During 1000 h at 0.2 mA cm ⁻² with overpotential ≈25 mV	99.61% within 1000 cycles at 1 mA cm ⁻²	[25]
Zn ²⁺ flux	Homogeneous zinc fluoride (ZnF ₂) layer with high Zn ²⁺ conductivity	Zn ²⁺ conductor	2 M ZnSO ₄	During 600 h at 10 mA cm ⁻² with plating/stripping overpotential ≈56.4 mV	99.5% within 1000 cycles at 1 mA cm ⁻²	[26]
Zn ²⁺ flux	zinc ion conductor (ZnyO _{1-x} F _x)	Zn ²⁺ conductor	2 M ZnSO ₄	1000 h at 1.0 mA cm ⁻² with overpotential of 20.4 mV	100% after 100 cycles at 1 mA cm ⁻²	[27]
Zn ²⁺ flux	Zn-Phytic acid (PA) interlayer	Chemical co-ordination	2 M ZnSO ₄	2000 h at 0.5 mA cm ⁻² with voltage hysteresis of ≈20 mV	99.9% over 800 cycles at 2 mA cm ⁻²	[32]
Zn ²⁺ flux	Thermoplastic polyurethane (TPU) fiber matrix and Zn-alginate (ZA) hybrid interface (TPZA)	Chemical co-ordination	2 M ZnSO ₄	>1800 h, 1200 and 500 h at 2 mA cm ⁻² , 5 mA cm ⁻² and 10 mA cm ⁻² with stable voltage curve	98.63%, 99.05%, and 99.47% at 2 mA cm ⁻² , 5 mA cm ⁻² and 10 mA cm ⁻² after 300, 300 and 150 cycles	[33]

Table 1. continued

Modulation strategies	Artificial interphase materials	Material properties	Electrolyte	Cyclic performance	CE	Refs.
Zn ²⁺ flux	poly(anionic 3-sulfopropyl methacrylate potassium salt) (PSPMA) interface	Chemical co-ordination	2 M ZnSO ₄	More than 1000 h at 1 mA cm ⁻² and 2500 h at 10 mA cm ⁻² with voltage hysteresis of 35 mV and 53 mV	99.9% over 900 cycles at 5 mA cm ⁻²	[34]
Zn ²⁺ flux	Zn _x -diethylenetriaminepenta(methylene-phosphonic acid) (Zn _x -DTPMP) interface	Chemical co-ordination	2 M ZnSO ₄	Voltage hysteresis of 19.9, 23.7, 32.5, 58.2, and 93.2 mV under various current densities (0.5 mA cm ⁻² , 1 mA cm ⁻² , 2 mA cm ⁻² , 5 mA cm ⁻² , 10 mA cm ⁻²)	100% after 120 cycles at 1 mA cm ⁻²	[35]
Zn ²⁺ flux	Zn-Al alloy films	Insulating	2 M ZnSO ₄	3000 h at 1 mA cm ⁻² with voltage hysteresis of 48.3 mV	99.25% after 400 cycles at 2 mA cm ⁻² and 99.13% at 5 mA cm ⁻² after 480 cycles	[37]
Zn ²⁺ flux	Zn interface in ULE	Positive charge repulsion	ULE (3 M Zn-(OTf) ₂ +1 M urea + 0.3 M LiOAc)	435 h with a capacity of 1087.5 mAh cm ⁻² at 5 mA cm ⁻²	99.7% after 600 h at 4.8 mA cm ⁻²	[39]
Zn ²⁺ flux	NVP (Na ₃ V ₂ (PO ₄) ₃) @AC (amorphous carbon) @rGO (reduced graphene oxide)	Positive charge repulsion	1 M Ca(OTf) ₂ + 1 M Zn(OTf) ₂ (1+1 CZH)	630 h at 2 mA cm ⁻²	99% over 500 cycles at 1 mA cm ⁻²	[40]
Zn ²⁺ flux	Zn interface in 1 M TC-ZC	Positive charge repulsion	Triethylmethyl-1+1 M ZnCl ₂ + ammonium chloride (TC-ZC)	2145 h at 1.0 mA cm ⁻² with overpotential of 25 mV	97.7% over 750 cycles at 1 mA cm ⁻²	[41]
HER intermediates	CuN ₃ -C ₃ N ₄ anticatalytic interface	Regulating adsorption of H* and H ₃ O ⁺ intermediates	2 M ZnSO ₄	Over 1300 h at 1 mA cm ⁻² with cycling reversibility	99.7% after 5500 cycles at 1 mA cm ⁻²	[45]
HER intermediates	Pb-containing interface on Zn (Zn@Pb)	Regulating adsorption of H* and H ₃ O ⁺ intermediates	1 M ZnSO ₄ + 0.1 M H ₂ SO ₄	Over 400 h at 4 mA cm ⁻² without voltage fluctuations	99% after 350 cycles at 5 mA cm ⁻²	[46]
HER intermediates	ZnMoO ₄ layer on the Zn anode (Zn@ZnMoO ₄)	Regulating adsorption of H* and H ₃ O ⁺ intermediates	3 M ZnSO ₄ + 0.1 M MnSO ₄	10000 cycles at 1 mAh cm ⁻² under 10 mA cm ⁻²	–	[47]
Anions	Zeolite protective coating layer	Electrostatic shielding	2 M ZnSO ₄	More than 2200 h at 1 mA cm ⁻² with an overpotential ≈ 17 mV	99.5% after 255 cycles at 1 mA cm ⁻²	[49]
Anions	hydroxymethyl Zn phosphates (Zn(O ₃ PCH ₂ OH, ZnOPC)	Electrostatic shielding	2 M ZnSO ₄	1000 h at 5 mA cm ⁻² with polarization potentials of 73.79 mV; 700 h at 10 mA cm ⁻² with polarization potentials of 105.02 mV	99.5% after 1000 cycles at 5 mA cm ⁻²	[50]
Anions	Cellulose nanofiber (CNF)/MXene	Electrostatic shielding	3 M Zn-(CF ₃ SO ₃) ₂	1200 h at 1 mA cm ⁻² with overpotential ≈ 60 mV	99.43% after 200 h at 5 mA cm ⁻²	[51]
Anions	β-cyclodextrin (β-CD)@ClO ₄ ⁻	Negative charge	1 M Zn(ClO ₄) ₂ with β-CD additive	Over 1200 h at 1 mA cm ⁻² ; over 350 h at 5 mA cm ⁻²	97.6% after 530 cycles at 5 mA cm ⁻²	[52]
Anions	Carbon dots	Negative charge	2 M ZnSO ₄ + 20% DMF	Over 4000 h at 1 mA cm ⁻² with polarization voltage of 50 mV	98.6% after 20 cycles at 1 mA cm ⁻²	[54]
Anions	Concentration gradient (ACG)-assisted solid-electrolyte interphase (SEI)	Negative charge	2 M ZnSO ₄	Over 2200 h at 3 mA cm ⁻² with stable polarization voltage	99.8% over 2000 cycles at 1 mA cm ⁻²	[55]

Table 1. continued

Modulation strategies	Artificial interphase materials	Material properties	Electrolyte	Cyclic performance	CE	Refs.
Anions	SiO ₂ reinforced-sodium alginate (SA) hybrid film	Guest species aggregation	2 M ZnSO ₄	Over 3000 h at 2 mA cm ⁻² with a voltage hysteresis of \approx 47.6 mV	99.8% over 2000 cycles at 2 mA cm ⁻²	[9]
Anions	Electrical double layer (EDL) containing saccharin (Sac) derived anions	Guest species aggregation	2 M ZnSO ₄ + 0.5 g L ⁻¹ Sac	Over 550 h at 10 mA cm ⁻² with stable polarization voltage	99.8% over 300 cycles at 2 mA cm ⁻²	[60]
Anions	Solvation-induced interphases with methylammonium acetate (MAAC)	Deriving in situ layers	2 M ZnOTF + 5 wt % MAAC	1700 h at 0.5 mA cm ⁻² /0.5 mAh cm ⁻² with an average overpotential of 40 mV	99.5% for 700 cycles (1400 h) at 0.5 mA cm ⁻² /0.5 mAh cm ⁻²	[64]
Anions	SEI with N-methylpyrrolidone (NMP) participation	Deriving in situ layers	2 M ZnSO ₄ + 5% NMP	Over 1100 h and 800 h together at 0.5 mA cm ⁻² /0.5 mAh cm ⁻² and 1 mA cm ⁻² /1 mAh cm ⁻² with minimal change in overpotential	99.5% for more than 200 cycles at 1 mA cm ⁻² /1 mAh cm ⁻²	[65]
Anions	SEI with tetramethylurea (TMU) participation	Deriving in situ layers	4 M Zn(OTF) ₂ + 0.25 M TMU	Over 1600 h at 5 mA cm ⁻² /2.5 mAh cm ⁻² with smooth voltage polarization	99.5% across 1200 cycles at 0.5 mA cm ⁻² /0.5 mAh cm ⁻²	[66]

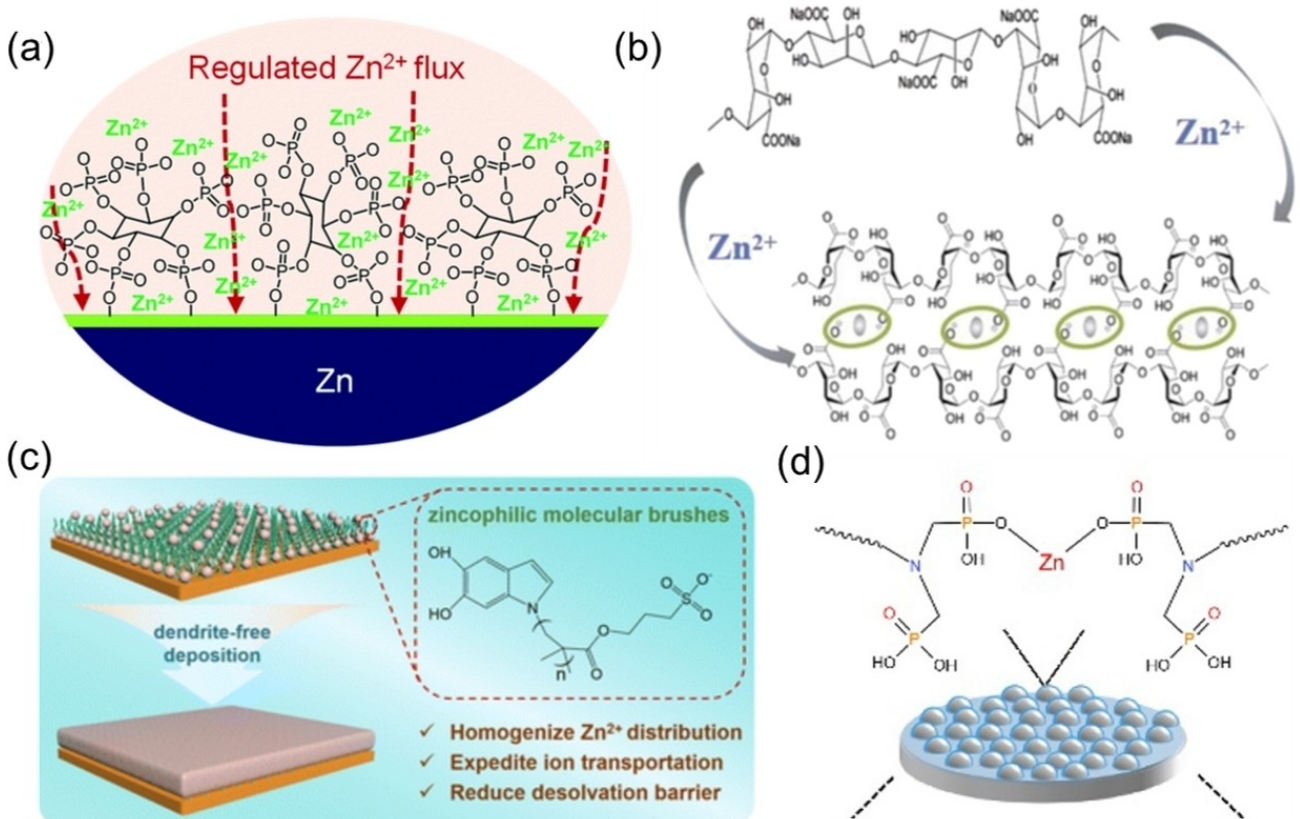


Figure 3. a) Schematic diagram of zinc deposition on Zn-PA@Zn. Reproduced with permission from Ref. [32]. Copyright (2022) Royal Society of Chemistry. b) Cross-linking mechanism formation of chemical coordination between Zn and alginate. Reproduced with permission from Ref. [33]. Copyright (2022) Wiley-VCH. c) Schematic diagram of PSPMA@Zn in inhibiting dendrite growth. Reproduced with permission from Ref. [34]. Copyright (2023) Royal Society of Chemistry. d) Schematic diagram of Zn anode surface modification layer formed by the chelate DTPMP and Zn²⁺. Reproduced with permission from Ref. [35]. Copyright (2022) American Chemical Society.

regulate the distribution of Zn²⁺ flux and exhibit excellent stability. In Figure 3d, the nano-structured Zn_x-diethylenetriami-

nepenta (methylene-phosphonic acid) (Zn_x-DTPMP) coating has hydrophobic (-CH₂)₂N- groups and zincophilic groups

($-Zn-O-P=O$), which effectively inhibit the transport of water molecules and serve as favorable sites for Zn^{2+} adsorption.^[35]

With coordination interaction, artificial interface layer results in ultra-fast Zn^{2+} transport and optimized Zn^{2+} flux distribution near the Zn anode.

2.5. Electrostatic shielding

2.5.1. Insulating

Based on electrostatic shielding, artificial layer can effectively prevent the rapid acquisition of electrons and inhibit the deposition of Zn^{2+} on the tip, thus optimizing Zn^{2+} flux.^[36]

In Figure 4a, an electrostatic shield with appropriate Al content can significantly optimize the distribution of Zn^{2+} flux and avoid excessive Zn^{2+} accumulation, thereby inhibiting the formation of dendrites for prolonged lifetime of Zn anode.^[37]

In brief, introducing insulating layer can effectively regulate the electric field around the nucleation site on the Zn anode, inhibit tip accumulation and induce uniform Zn plating, thus reducing dendrite formation and enhancing the cycle life.^[38]

2.5.2. Positive charge repulsion

The adsorbed cations that are mutually repulsive with Zn^{2+} on the tip surface can redistribute Zn^{2+} flux and local current density through electrostatic repulsion, leading to suppressed Zn dendrites.

In Figure 4b, the positively charged Li^+ in aqueous electrolyte accumulates on the dendrite surface due to the charge interaction, which has an inhibitory effect on the Zn^{2+} plating

at the tip.^[39] Additionally, the electrostatic shield layer formed by accumulated Ca^{2+} on the Zn tip effectively prevents Zn^{2+} from approaching the tip and induces Zn^{2+} flux to concentrate on the flat area (Figure 4c).^[40] Similarly, TMA^+ has a positive charge shielding effect, which inhibits the formation of Zn dendrites and further improves the Zn deposition (Figure 4d).^[41]

Consequently, the introduction of guest cations in the electrolyte not only increases the number of charge carriers to improve the rate performance, but also aggregates on the tip to form an electrostatic shielding layer for suppressing tip effect.

3. HER Intermediates (H_3O^+ and H^*)

Anti-catalytic Properties

The low-cost and nonflammable properties of aqueous electrolytes facilitate sustainable electrochemical energy storage technologies.^[42] However, the HER induced by the electrolysis of water leads to battery safety issues and decreases in CE and energy density. Discussing the mechanism of water electrolysis on the electrode from the perspective of catalysis is expected to provide new insights into the suppression of HER. In general, materials that exhibit inherently high overpotentials and higher activation energies towards HER are defined as anticatalysts.^[43] To achieve feasible anticatalytic strategies, anticatalytic materials that used for regulating the elementary steps of HER (H^* intermediate adsorption and H_2 gas desorption) were introduced into the Zn surface. Since the basic steps of HER are affected by the binding energy between the intermediate and the electrode surface, the binding energy serves as a key

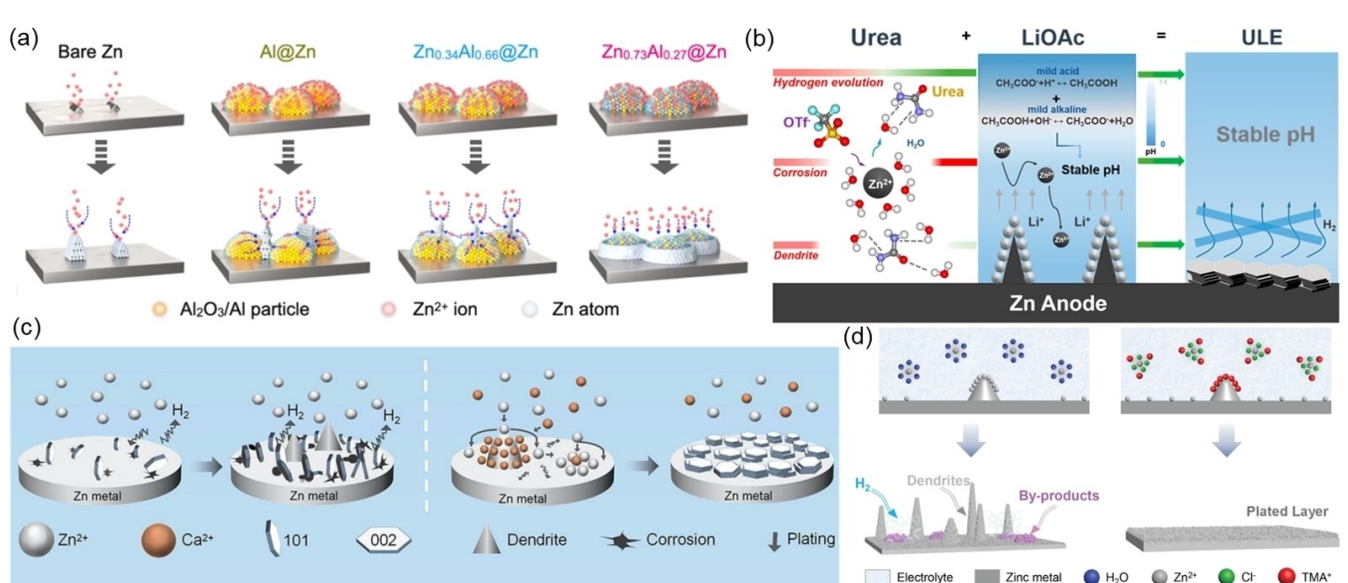


Figure 4. Illustration of a) Zn deposition on bare Zn, Al@Zn, $Zn_{0.34}Al_{0.66}@Zn$, and $Zn_{0.73}Al_{0.27}@Zn$. Reproduced with permission from Ref. [37]. Copyright (2022) American Chemical Society. b) The synergistic effect of ULE in improving the stability of zinc anode. Reproduced with permission from Ref. [39]. Copyright (2023) American Chemical Society. Mechanism of zinc deposition optimized by c) 1+1 CZH electrolyte and d) TMA^+ . Reproduced with permission from Ref. [40]. Copyright (2023) Science China Press. Published by Elsevier B.V. and Science China Press. Reproduced with permission from Ref. [41]. Copyright (2021) Wiley-VCH.

indicator to evaluate the anti-catalytic performance of electrode materials.^[43,44]

In general, the construction of anti-catalytic interface not only decreases the activity of HER reaction sites, but also has the effect of regulating Zn²⁺ flux. In recent, various multifunctional protection materials with anti-catalytic performance and can significantly improve the performance of ZIBs have aroused much attention.

In Figure 5a and b, the constructed CuN₃-C₃N₄ layer has a stabilizing effect on H₃O⁺ near the surface and can regulate the adsorption energy of H* intermediate, thus significantly inhibited HER reactivity. Moreover, inhibiting HER can delay the formation of ZHS, which not only effectively extended the cycle life of ZIBs, but also improved the safety.^[45]

Due to the lower HER catalytic activity, Pb species shows higher Gibbs free energy of hydrogen adsorption than that of Zn metal, which increases the H₂ escape energy barrier (Figure 5c). Consequently, the Pb-containing interface prevented H⁺ from reaching the Zn surface and inhibited HER.^[46]

In Figure 5d, ZnMoO₄ has a higher Gibbs free energy of H (adsorbed hydrogen atoms) than Zn, which suppressing the occurrence of HER. Moreover, it has stronger interaction and binding energy with Zn²⁺ than Zn (001), and its O atom is the preferred adsorption site for Zn²⁺.^[47]

In brief, the interface layer modification can affect the binding energy with hydrogen atoms, and effectively regulate the adsorption behavior of active intermediate H* and desorption behavior of H₂*, which ultimately inhibit HER. The suppression of HER can undoubtedly improve the safety of practical applications.^[48]

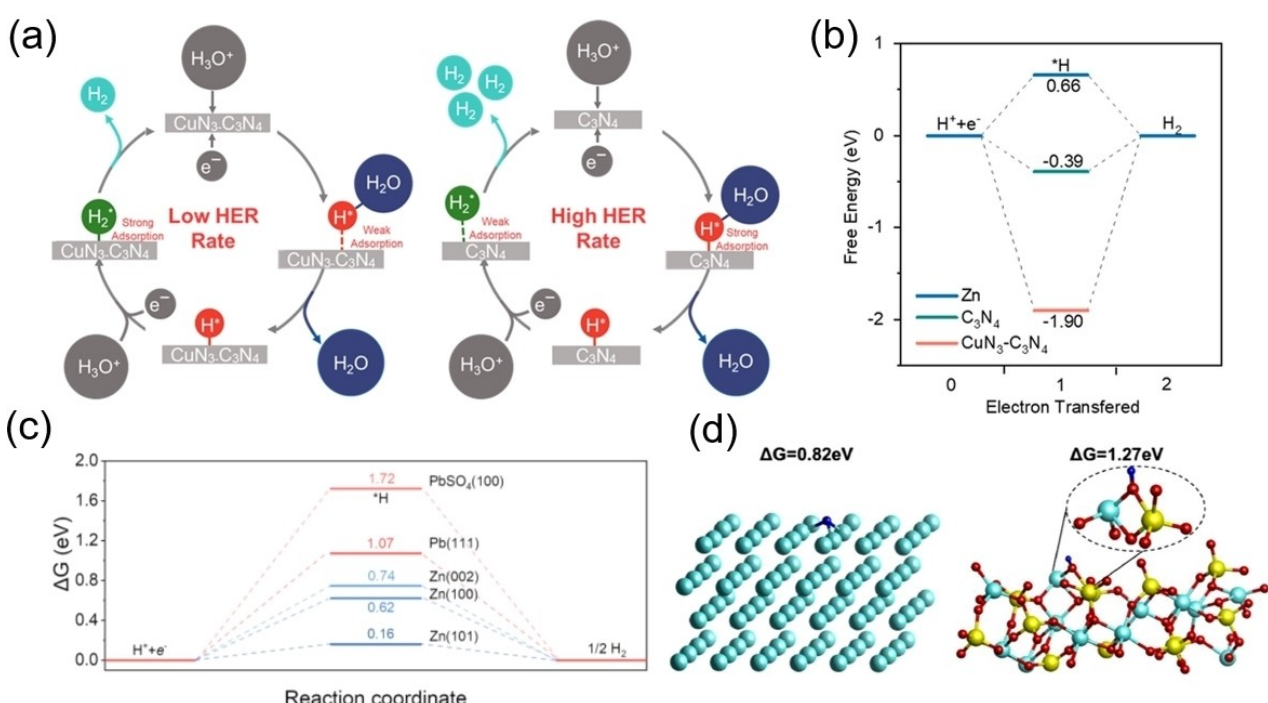


Figure 5. (a) The HER mechanism of CuN₃-C₃N₄ (left) and C₃N₄ (right). (b) The adsorption free energy of H species on Zn, C₃N₄, and CuN₃-C₃N₄.^[45] Reproduced from Ref. [45] Copyright (2023), with permission from American Chemical Society. (c) The Gibbs free energy of H⁺ on the surface of PbSO₄(100), Pb(111), Zn(002), Zn(100), and Zn(101).^[46] Reproduced from Ref. [46] Copyright (2023), with permission from Wiley-VCH GmbH. (d) The hydrogen evolution barrier of Zn (001) (left) and ZnMoO₄ (right).^[47] Reproduced from Ref. [47] Copyright (2021), with permission from Elsevier B.V. All rights reserved.

4. The Regulation of Anions in Electrolyte

In addition to achieving smooth Zn deposition by cation regulation, the application of anti-catalytic interface effectively impacts the adsorption/desorption behaviors of HER intermediates and alleviates HER-related side reactions. Together with HER, the accumulation of insulating ZHS by-products also limit the reversibility of Zn electrodes. The regulation of anions including host anions (mainly sulfate ions) and guest anions from additives in electrolyte has recently attracted intensive attention as an accessible strategy to protect Zn anodes.

4.1. Electrostatic shielding

The sulfate anions on the anode surface directly participate in the generation of by-products, thus the suppression of by-products can be realized by blocking the contact between sulfate ions and the Zn electrode. Taking advantages of the smaller pore size than sulfate anions, artificial layer with the restricted structure has been designed to repel the penetration of sulfate groups, such as zeolite (Figure 6a),^[49] and hydroxymethyl Zn phosphates (ZnO₃PCH₂OH, ZnOPC) (Figure 6b).^[50] Figure 6a demonstrates the precise cation and anion sieving ability of Zn-exchanged zeolite. In addition, the strong interaction between Zn²⁺ and O facilitates the de-solvation process and induces uniform Zn deposition based on a 3D diffusion mechanism.^[49]

In addition to the size effect, the hydrated CF₃SO₃⁻ can be blocked by cellulose nanofiber (CNF)/MXene composite mem-

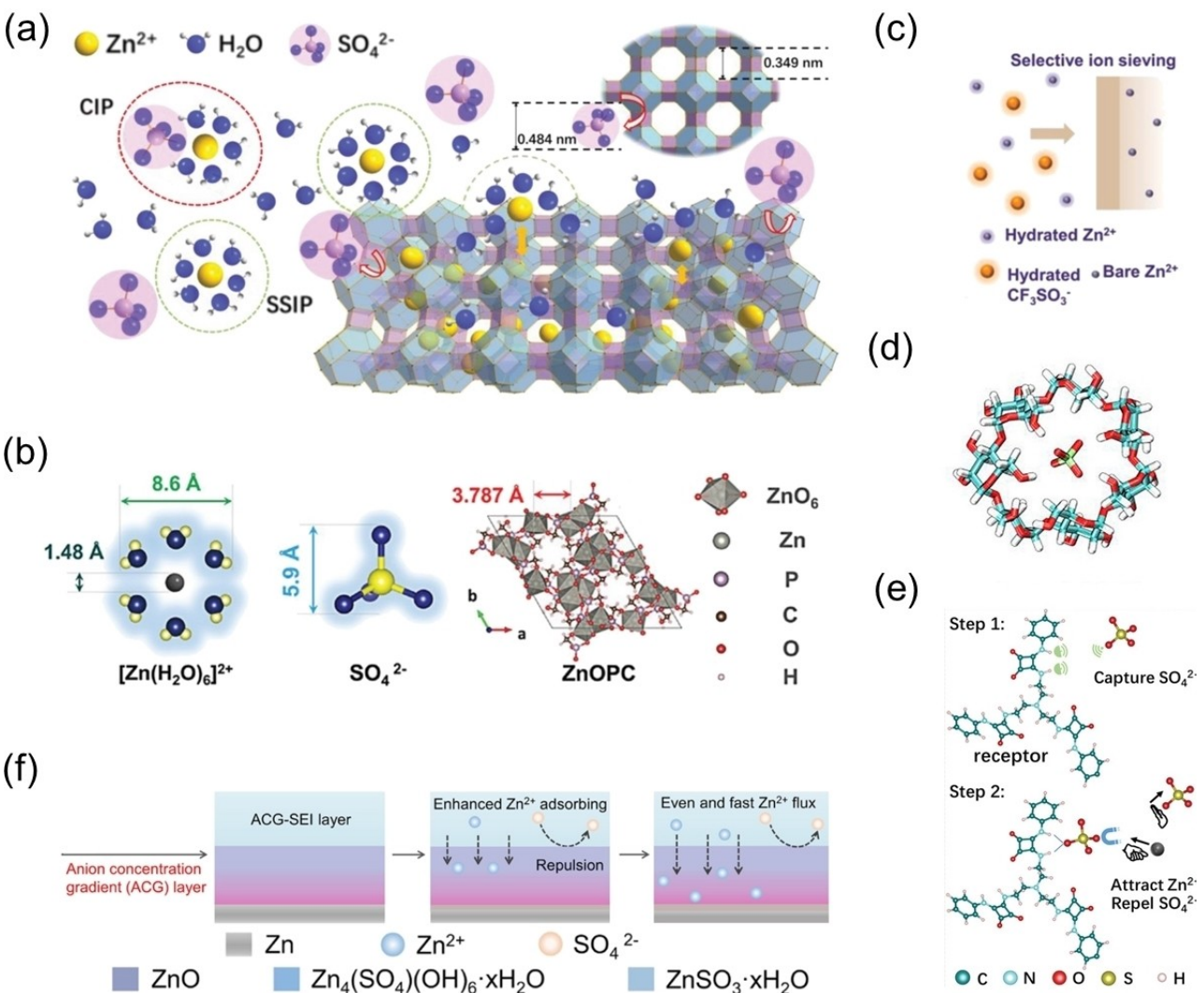


Figure 6. a) The scheme of ion transport in ZnA artificial interface. Reproduced with permission from Ref. [49]. Copyright (2023) Wiley-VCH. b) The illustration of ion sizes of hydrated Zn^{2+} and SO_4^{2-} , and crystal structure of ZnOPC. Reproduced with permission from Ref. [50]. Copyright (2022) Wiley-VCH. c) Schematic diagram of the blocking function of the CNF/MXene membrane for hydrated $CF_3SO_3^-$ anions and water. Reproduced with permission from Ref. [51]. Copyright (2023) Wiley-VCH. d) Encapsulating ClO_4^- in β -CD via anion-trap. Reproduced with permission from Ref. [52]. Copyright (2022) Wiley-VCH. e) The enhanced Zn^{2+} adsorbing and anion repulsion in the ACG layer. Reproduced with permission from Ref. [54]. Copyright (2023) Elsevier B.V. f) The role illustrations of the constructed SR and the resulting SR- SO_4^{2-} . Reproduced with permission from Ref. [55]. Copyright (2022) American Chemical Society.

brane because the deprotonated C–OH and C–COOH in cellulose preferentially adsorb Zn^{2+} rather than anions (Figure 6c).^[51] To mitigate anions coupling with Zn^{2+} and disturbing Zn^{2+} migration, Mai et al.^[52] proposed an interesting “anion-trap” strategy to immobilize ClO_4^- anions in β -cyclodextrin (β -CD), shown in Figure 6d, thereby facilitating Zn^{2+} transport and inducing Zn deposition along (002). In brief, anion regulation is often accompanied by cation modulation, synergistically enabling high-performance Zn anodes.

4.2. Negative charge

As another commonly used method to repel solute anions, an artificial interface with negative charges is introduced on the Zn surface, resulting in electrostatic repulsion between SO_4^{2-} and

the protective material. The electrostatic effect of artificial layer hinders the anion from penetrating to the Zn surface. For example, an in situ anion concentration gradient (ACG)-assisted artificial interphase was constructed on the Zn surface by reacting with sulfonic acid polymer.^[53] The electronegative $-SO_3^-$ groups in the artificial layer provide active sites to facilitate Zn^{2+} diffusion and repel sulfate (Figure 6e). In addition, a carbon dot (CDs) layer was developed to enhance the performance of Zn anodes,^[54] in which the $-SO_3^-$ groups can effectively bond with Zn^{2+} to repel SO_4^{2-} .

Interestingly, sulfate ions in the electrolyte can also be modulated by multifunctional SO_4^{2-} receptors (denoted as SR). As displayed in Figure 6f, the $-NH-$ groups in SR have high affinity with SO_4^{2-} , which can bridge and bind SO_4^{2-} via forming $-NH-O$ bonds.^[55] After capturing SO_4^{2-} , the corresponding negatively charged SR artificial layer not only distributes Zn^{2+}

for smooth Zn deposition, but also repels the additional SO_4^{2-} in the electrolyte due to the electrostatic effect. What's more, the constructed SR and the resulting SR- SO_4^{2-} promote the Gibbs free energy of HER, preventing the occurrence of HER. In recent, an artificial layer of metal oxide, CeO_2 aerogel with abundant oxygen vacancies (VAG-Ce), was also used as ion sieve and SO_4^{2-} -capturer to protect Zn anode.^[56] The exposed oxygen vacancies in the interface can effectively capture SO_4^{2-} , bringing about a negatively charged interface to attract Zn^{2+} and repel the remaining SO_4^{2-} anions.

4.3. Guest species aggregation

It is widely accepted that water molecules occupy the inner layer of the EDL to form an inner Helmholtz plane (IHP) when the Zn electrode is in contact with the electrolyte, resulting in serious side effects.^[57] On the outside of the water molecule layer, hydrated Zn^{2+} aggregates to form the outer Helmholtz plane (OHP).^[58]

To further investigate the existence and influence of anions in EDL, Yang et al.^[9] proposed and demonstrated that the IHP consists of water dipoles and SO_4^{2-} anions, and the hydrated Zn^{2+} cations can only approach OHP, as displayed in Figure 7a. In addition, some SO_4^{2-} anions are accompanied with hydrated Zn^{2+} cations to maintain charge neutrality. The free-water and

SO_4^{2-} anions will lead to the fatal side reactions, thus Zn anode protection can be achieved through the reconfiguration of the Helmholtz layer. Figure 7a exhibits that the SiO_2 reinforced-sodium alginate ($\text{SiO}_2@\text{SA}$) layer effectively regulate the species distribution in EDL. Specifically, the abundant carboxyl groups in SA are negatively charged, and repel the SO_4^{2-} ions from the Helmholtz layer. Furthermore, the carboxyl oxygen can preferentially coordinate with Zn^{2+} ions, accelerating the Zn^{2+} charge-transfer process, and the proportion of free water in EDL decreased from 57.3% to 17.5%.^[58] In recent, an additive named 1,4-dioxane (DX) was also reported to suppress side reactions by regulating the EDL structure.^[59] In addition, some studies have pointed out that the formation of SEI is highly correlated with the regulation of EDL.^[60] Therefore, investigating the EDL structure formed before cycling is crucial for establishing an artificial SEI that improves the Zn/electrolyte interface stability. As displayed in Figure 7b, saccharin (Sac) anions derived from the Sac electrolyte additive are preferentially adsorbed on the Zn surface, leading to a water-poor EDL without side reactions. More importantly, the sac anions on the electrode surface can be decomposed into an in situ artificial SEI during cell cycling, enabling uniform Zn^{2+} deposition and prolonged lifespan.

In brief, guest species aggregation provides an effective strategy for inhibiting water molecules from accumulating on the electrode surface, thereby suppressing side reactions.

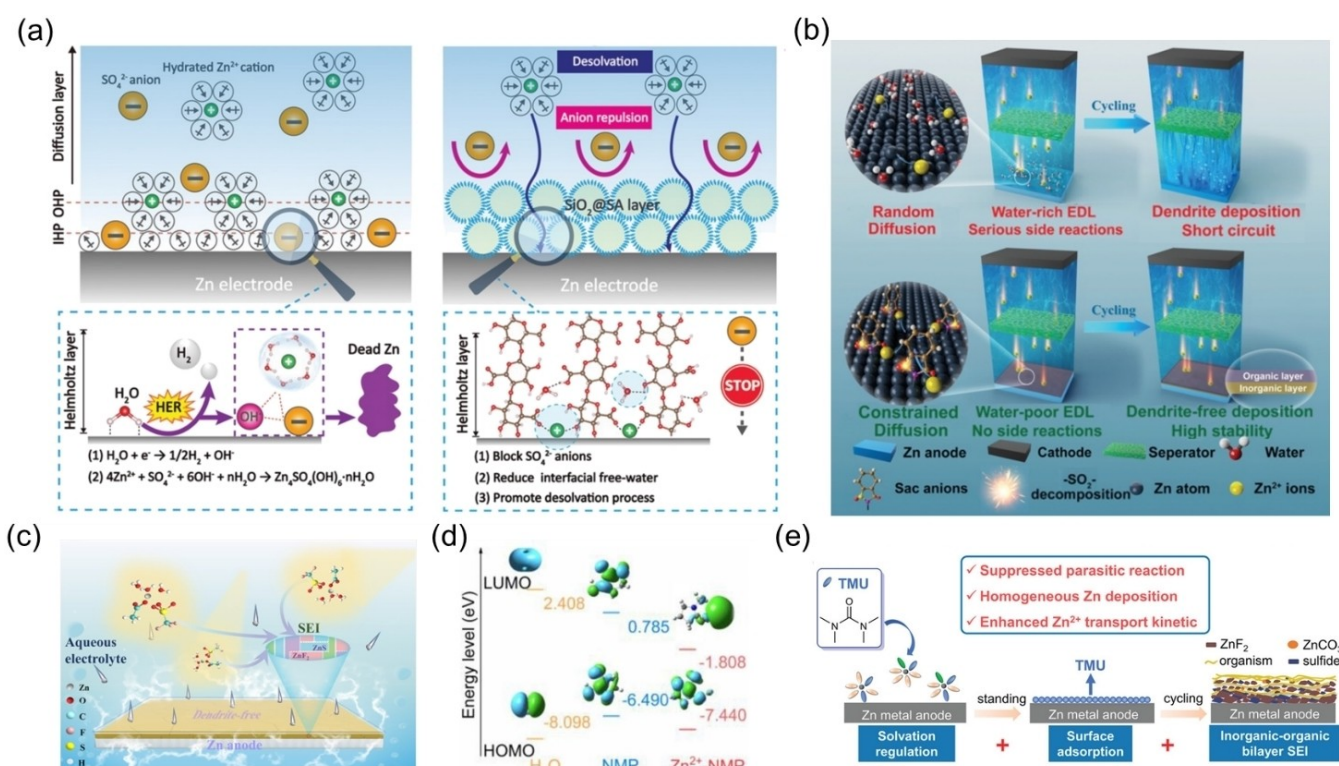


Figure 7. a) Schematic diagrams of the EDL structure for Zn and $\text{SiO}_2@\text{SA}$ coated Zn electrodes. Reproduced with permission from Ref. [9]. Copyright (2022) Wiley-VCH. b) The schematic illustration of the regulatory mechanism of Sac in the formation of water-poor EDL and in situ artificial SEI. Reproduced with permission from Ref. [60]. Copyright (2021) Wiley-VCH. c) The hybrid SEI in Zn/ZnOTF and MAAC electrolyte system. Reproduced with permission from Ref. [64]. Copyright (2023) American Chemical Society. d) The calculated results of HOMO and LUMO energy levels of different species. Reproduced with permission from Ref. [65]. Copyright (2022) Elsevier B.V. e) The protection mechanisms of TMU additive. Reproduced with permission from Ref. [66]. Copyright (2022) Wiley-VCH.

4.4. Ability to derive *in situ* layers

Different from reconstructing EDL, this section focuses on the derived *in situ* artificial interface. Notably, the functions of the two in protecting Zn anodes are not completely separated. The derived *in situ* layer contains adsorption-type and reaction-type protective layers. When additives are introduced into the electrolyte, the additive molecules or derivative anions with adsorption properties will be preferentially adsorbed on the surface of the Zn electrode to form adsorption-type protective layers, such as sulfolane molecules,^[61] monosodium glutamate,^[62] sodium tartrate,^[63] and etc. On the other hand, the formation of reaction-type artificial layers usually involves the anions, water, or additive molecules decomposition in aqueous electrolytes.

The anions that directly present in zinc salts, such as OTF⁻, contribute to the generation of a derived artificial SEI layer on the electrode surface. For example, the acetate anions (Ac⁻) in the methylammonium acetate (MAAC) additive can participate in and reconstruct the primary solvation sheath of Zn²⁺, resulting in an anion-enriched structure for reducing water activity and promoting the anion-derived artificial SEI.^[64] In Figure 7c, the OTF⁻ and Ac⁻ anions are preferentially adsorbed on the Zn surface, and the OTF⁻ anions can be electroreduced during cycling, constructing a hybrid SEI.

In addition to anions from conventional electrolytes, the *in situ* layer could form if the additives have lower lowest unoccupied molecular orbital (LUMO) levels than water. Due to the high donor number and strong electron-donating ability, N-methylpyrrolidone (NMP) was selected as an electrolyte additive to simultaneously stabilize the Zn anode and V₆O₁₃·H₂O cathode.^[65] In Figure 7d, the LUMO levels of both NMP and Zn²⁺-NMP complex are lower than those of water, implying that they are more easily decomposed to form artificial interface during Zn reduction. Moreover, the highest occupied molecular orbital (HOMO) energy level of NMP is highest, which means the largest tendency to guide cathode electrolyte interphase (CEI) formation on the cathode surface during oxidation. In such way, the stability of both anode and cathode is enhanced at the same time. Similarly, in Figure 7e, tetramethylurea additive restructure the Zn²⁺ solvation sheath together with OTF⁻ anions and derive a robust inorganic-organic SEI composed of ZnF₂ and zincophilic amide components.^[66]

5. Summary and Perspective

Aqueous Zn-ion batteries are considered to be low-cost, high-safety batteries and have broad application prospects in large-scale energy storage. The electrochemical performance of Zn-ion batteries is closely related to the stability and reversibility of metallic Zn anodes. To achieve high-performance Zn metal anodes without no dendrites and side reactions, many attempts have been made to develop advanced artificial electrode/electrolyte interfaces. In this review, we summary the modulation strategies in terms of Zn artificial interface, including the regulation of Zn²⁺ flux, HER intermediates (H₃O⁺ and H^{*}) and

anions in the electrolytes, aiming to provide an unprecedented design reference for achieving multi-level and high-performance Zn anode interfaces. The protection materials and electrochemical performance of different anion/cation modulation strategies has been presented in Table 1. Different desired functions can be achieved by adjusting the distribution of ionic groups. For example, regulating Zn²⁺ flux can effectively avoid Zn dendrites produced by uneven Zn deposition; and HER can be suppressed by adjusting HER intermediates. In addition, anions regulation strategies can not only reduce the generation of by-products by restricting reactants, but also reconstruct EDL or SEI components. Zn²⁺ flux regulation can be achieved by constructing pore structure, layered structure, or Zn²⁺ conductor layers, as well as based on chemical coordination, insulating and positive charge repulsion. In addition, the construction of anti-catalytic interface can effectively decrease the activity of HER reaction sites for suppressing HER. Regulatory strategies for anions including restricted structure or groups, negative charge, guest species aggregation, and deriving *in situ* layers on the Zn surface. By the systematically summarizing and discussing of cation and anion modulation strategies, we accurately grasp the development trend and research direction of the ideal artificial Zn/electrolyte interface, which can guide researchers to further improve the performance, and practicality.

To sum up, the following noteworthy points and perspectives are expected to guide the further research orientation to meet the requirement of multi-level and high-performance artificial Zn interfaces.

(1) Design composite multifunctional interfaces: Applying artificial layers with specific properties can effectively regulate cations and anions in ZIBs. As for the regulation of Zn²⁺ flux, pore structure and layered structure materials provide steric confinement effect to redistribute Zn²⁺ and avoid Zn²⁺ aggregation during Zn ion transport. In addition, Zn²⁺ conductor enables accelerated Zn²⁺ migration due to its own lattice. The chemical coordination between the functional groups in the artificial layer and Zn²⁺ facilitates the Zn²⁺ transportation and induces uniform Zn deposition. Moreover, the simple insulating coating and positively charged interface brings about a protective barrier, thus repelling Zn²⁺ and avoiding accumulating. With unique anti-catalytic properties, the constructed artificial interphase can regulate the adsorption behavior of HER intermediates (H₂^{*} and H^{*}) that directly participate in HER process. In addition, the migration of sulfate anions (from the electrolyte to the surface of the Zn metal anode) can be blocked by restricted structures or groups and electrostatic repulsion, thereby avoiding the formation of ZHS by-products. Furthermore, the water-poor EDL structure can be reconstructed on the Zn surface via guest species aggregation. In addition to the ions in the conventional electrolyte, if the introduced additives and their derived anions have adsorption characteristics and preferential decomposition ability, exhibiting strong adsorption energy and low LUMO energy level, it will be possible to form an *in-situ* artificial layer on the surface of the Zn

electrode to enhance the lifespan. Considering the above-mentioned properties and functions, designing composite interfaces combining unique structures, coordination chemical groups, anti-catalytic capacity, etc. for high-performance Zn anodes is expected to become a research hotspot in the future.

- (2) Interface structure design for multi-level regulation: In addition to investigating the synergy between artificial layer components (noteworthy point 1), the structural design, such as double-layer structure and sandwich structure, can also bring fresh insights into the realization of multi-level regulation. For example, the inner layer is composed of inorganic substances that facilitate the transport of zinc ions, and the outer layer is composed of self-healing materials that can adapt to volume changes.
- (3) Focus on species that directly triggers side effects: Current research involving artificial protective layers is mainly focused on the regulation of Zn^{2+} flux and the reduction of water activity. Besides these, the regulation of H_3O^+ species and H^* intermediates, and anions in the battery system that is often overlooked needs to receive more attention in future research.
- (4) The balance between the protection effect and fast kinetics: Notably, although the construction of an artificial interface has been proven to be effective in improving the reversibility of Zn anodes, its limitations still need to be paid attention to. As for protection materials that induce Zn^{2+} flux via pore structure, Maxwell-Wagner polarization, and electronic insulating are hampered by micrometer-scale thickness and relatively low ion transfer kinetics.^[67] Building nanoscale coatings with advanced construction techniques can provide new inspiration for addressing this limitation.^[68] In addition, selecting artificial layer with fast Zn^{2+} transmission capacity like MMT-Zn is also helpful.^[69] What's more, developing protection layer with multilayered gradients is of significance for achieving ideal interface.^[67] Gradient structures can provide synergistic effects, taking advantage of both electronically insulating and ionically conducting layers. For example, the outer component of the artificial layer can be used to block electron channels and thus suppress the HER tendency, while the inner component with high Zn^{2+} conductivity can further homogenize the Zn^{2+} flux and eliminate the "tip effect".^[67]
- (5) In-depth of computation and characterization: Future research should focus on the development of theoretical models, such as dendrite growth models. In addition, the quantification and in-situ detection of HER and by-products need to be continuously deepened, and an in-depth understanding of the reaction mechanism is more conducive to overcoming the challenges of Zn anodes.

Acknowledgements

This work was supported by the National Natural Science Foundation of China (Grant Nos. 22075028 and 22209013), China Postdoctoral Science Foundation (Grant No.

2022M710365), Project of Cooperation of the Chinese Academy of Engineering and Local Governments (Grant No. 2021-FJ-ZD-2), and the BIT Research and Innovation Promoting Project (Grant No. 2022YCXZ034).

Conflict of Interests

The authors declare no conflict of interest.

Keywords: aqueous Zn-ion batteries (ZIBs) • Zn anodes • artificial Zn/electrolyte interface • cation and anion modulation

- [1] a) Y. Li, F. Wu, Y. Li, M. Liu, X. Feng, Y. Bai, C. Wu, *Chem. Soc. Rev.* **2022**, 51, 4484–4536; b) H. Gao, N. S. Grundish, Y. Zhao, A. Zhou, J. B. Goodenough, *Energy Mater. Adv.* **2021**, 2021; c) Z. Hu, R. Zhao, J. Yang, C. Wu, Y. Bai, *Energy Storage Mater.* **2023**, 59, 102776.
- [2] a) S. Chen, Y. Ying, L. Ma, D. Zhu, H. Huang, L. Song, C. Zhi, *Nat. Commun.* **2023**, 14, 2925; b) J. Yang, R. Zhao, Y. Wang, Z. Hu, Y. Wang, A. Zhang, C. Wu, Y. Bai, *Adv. Funct. Mater.* **2023**, 33, 2213510; c) A. Zhang, R. Zhao, Y. Wang, J. Yang, C. Wu, Y. Bai, *Energy Environ. Sci.* **2023**, 16, 3240–3301.
- [3] Q. Ni, H. Jiang, S. Sandstrom, Y. Bai, H. Ren, X. Wu, Q. Guo, D. Yu, C. Wu, X. Ji, *Adv. Funct. Mater.* **2020**, 30, 2002825.
- [4] a) H. Ge, X. Feng, D. Liu, Y. Zhang, *Nano Research Energy* **2023**, 2, e9120039; b) B. Zhou, B. Miao, Y. Gao, A. Yu, Z. Shao, *Small* **2023**, 2300895.
- [5] a) R. Li, Y. Du, Y. Li, Z. He, L. Dai, L. Wang, X. Wu, J. Zhang, J. Yi, *ACS Energy Lett.* **2023**, 8, 457–476; b) W. Nie, H. Cheng, Q. Sun, S. Liang, X. Lu, B. Lu, J. Zhou, *J. Power Sources* **2022**, 522, 230994; c) Z. Xing, C. Huang, Z. Hu, *Coord. Chem. Rev.* **2022**, 452, 214299.
- [6] a) J. Yang, R. Zhao, Y. Wang, Y. Bai, C. Wu, *Energy Mater. Adv.* **2022**, 2022; b) Z. Yu, Y. Cui, Z. Bao, *Cell Rep. Phys. Sci.* **2020**, 1, 110119.
- [7] a) M. Gopalakrishnan, S. Ganesan, M. T. Nguyen, T. Yonezawa, S. Praserttham, R. Pornprasertsuk, S. Kheawhom, *Chem. Eng. J.* **2023**, 457, 141334; b) R. Qin, Y. Wang, L. Yao, L. Yang, Q. Zhao, S. Ding, L. Liu, F. Pan, *Nano Energy* **2022**, 98, 107333; c) W. Du, J. Yan, C. Cao, C. C. Li, *Energy Storage Mater.* **2022**, 52, 329–354.
- [8] C. Mao, Y. Chang, X. Zhao, X. Dong, Y. Geng, N. Zhang, L. Dai, X. Wu, L. Wang, Z. He, *J. Energy Chem.* **2022**, 75, 135–153.
- [9] Y. Yang, H. Hua, Z. Lv, M. Zhang, C. Liu, Z. Wen, H. Xie, W. He, J. Zhao, C. C. Li, *Adv. Funct. Mater.* **2023**, 33, 2212446.
- [10] Y. Wang, Z. Deng, B. Luo, G. Duan, S. Zheng, L. Sun, Z. Ye, J. Lu, J. Huang, Y. Lu, *Adv. Funct. Mater.* **2022**, 32, 2209028.
- [11] P. Zou, R. Zhang, L. Yao, J. Qin, K. Kisslinger, H. Zhuang, H. L. Xin, *Adv. Energy Mater.* **2021**, 11, 2100982.
- [12] L. Kang, M. Cui, F. Jiang, Y. Gao, H. Luo, J. Liu, W. Liang, C. Zhi, *Adv. Energy Mater.* **2018**, 8, 1801090.
- [13] J. Liu, C. Ye, H. Wu, M. Jaroniec, S.-Z. Qiao, *J. Am. Chem. Soc.* **2023**, 145, 5384–5392.
- [14] J.-L. Yang, J. Li, J.-W. Zhao, K. Liu, P. Yang, H. J. Fan, *Adv. Mater.* **2022**, 34, 2202382.
- [15] H. Sun, Y. Huyan, N. Li, D. Lei, H. Liu, W. Hua, C. Wei, F. Kang, J.-G. Wang, *Nano Lett.* **2023**, 23, 1726–1734.
- [16] C. Guo, J. Zhou, Y. Chen, H. Zhuang, Q. Li, J. Li, X. Tian, Y. Zhang, X. Yao, Y. Chen, S.-L. Li, Y.-Q. Lan, *Angew. Chem. Int. Ed.* **2022**, 61, e202210871.
- [17] a) E. Kim, I. Choi, K. W. Nam, *Electrochim. Acta* **2022**, 425, 140648; b) P. Xue, C. Guo, L. Li, H. Li, D. Luo, L. Tan, Z. Chen, *Adv. Mater.* **2022**, 34, 2110047.
- [18] X. Hu, Z. Lin, S. Wang, G. Zhang, S. Lin, T. Huang, R. Chen, L.-H. Chung, J. He, *ACS Appl. Energ. Mater.* **2022**, 5, 3715–3723.
- [19] Y.-M. Li, W.-H. Li, W.-Y. Diao, F.-Y. Tao, X.-L. Wu, X.-Y. Zhang, J.-P. Zhang, *ACS Appl. Mater. Interfaces* **2022**, 14, 23558–23569.
- [20] S. Jiao, J. Fu, M. Wu, T. Hua, H. Hu, *ACS Nano* **2022**, 16, 1013–1024.
- [21] C. Deng, X. Xie, J. Han, Y. Tang, J. Gao, C. Liu, X. Shi, J. Zhou, S. Liang, *Adv. Funct. Mater.* **2020**, 30, 2000599.
- [22] H. Yan, S. Li, Y. Nan, S. Yang, B. Li, *Adv. Energy Mater.* **2021**, 11, 2100186.
- [23] Y. Yang, C. Liu, Z. Lv, H. Yang, X. Cheng, S. Zhang, M. Ye, Y. Zhang, L. Chen, J. Zhao, C. C. Li, *Energy Storage Mater.* **2021**, 41, 230–239.

- [24] M. Liu, J. Cai, H. Ao, Z. Hou, Y. Zhu, Y. Qian, *Adv. Funct. Mater.* **2020**, *30*, 2004885.
- [25] Y. Liang, Y. Kou, Q. Hao, F. Chen, X. Chen, N. Li, *Electrochim. Acta* **2023**, *443*, 141928.
- [26] L. Ma, Q. Li, Y. Ying, F. Ma, S. Chen, Y. Li, H. Huang, C. Zhi, *Adv. Mater.* **2021**, *33*, 2007406.
- [27] S. Zhao, Y. Zhang, J. Li, L. Qi, Y. Tang, J. Zhu, J. Zhi, F. Huang, *Adv. Mater.* **2023**, *35*, 2300195.
- [28] Y. Mao, Z. Li, Y. Li, D. Cao, G. Wang, K. Zhu, G. Chen, *Chem. Eng. J.* **2023**, *461*, 141707.
- [29] a) X. Yang, W. Wu, Y. Liu, X.-X. Liu, X. Sun, *Chem. Eng. J.* **2023**, *460*, 141678; b) Z. Zhao, J. Zhao, Z. Hu, J. Li, J. Li, Y. Zhang, C. Wang, G. Cui, *Energy Environ. Sci.* **2019**, *12*, 1938–1949.
- [30] Q. Zhang, J. Luan, Y. Tang, X. Ji, H. Wang, *Angew. Chem. Int. Ed.* **2020**, *59*, 13180–13191.
- [31] M. Zhu, J. Hu, Q. Lu, H. Dong, D. D. Karnaushenko, C. Becker, D. Karnaushenko, Y. Li, H. Tang, Z. Qu, J. Ge, O. G. Schmidt, *Adv. Mater.* **2021**, *33*, 2007497.
- [32] H. Liu, J.-G. Wang, W. Hua, L. Ren, H. Sun, Z. Hou, Y. Huyan, Y. Cao, C. Wei, F. Kang, *Energy Environ. Sci.* **2022**, *15*, 1872–1881.
- [33] Q. Liu, Y. Wang, X. Hong, R. Zhou, Z. Hou, B. Zhang, *Adv. Energy Mater.* **2022**, *12*, 2200318.
- [34] H. Liu, Q. Ye, D. Lei, Z. Hou, W. Hua, Y. Huyan, N. Li, C. Wei, F. Kang, J.-G. Wang, *Energy Environ. Sci.* **2023**, *16*, 1610–1619.
- [35] H. Yu, Y. Chen, W. Wei, X. Ji, L. Chen, *ACS Nano* **2022**, *16*, 9736–9747.
- [36] X. Guo, Z. Zhang, J. Li, N. Luo, G.-L. Chai, T. S. Miller, F. Lai, P. Shearing, D. J. L. Brett, D. Han, Z. Weng, G. He, I. P. Parkin, *ACS Energy Lett.* **2021**, *6*, 395–403.
- [37] J. Zheng, Z. Huang, Y. Zeng, W. Liu, B. Wei, Z. Qi, Z. Wang, C. Xia, H. Liang, *Nano Lett.* **2022**, *22*, 1017–1023.
- [38] S.-B. Wang, Q. Ran, R.-Q. Yao, H. Shi, Z. Wen, M. Zhao, X.-Y. Lang, Q. Jiang, *Nat. Commun.* **2020**, *11*, 1634.
- [39] X. Feng, P. Li, J. Yin, Z. Gan, Y. Gao, M. Li, Y. Cheng, X. Xu, Y. Su, S. Ding, *ACS Energy Lett.* **2023**, *8*, 1192–1200.
- [40] S. Zhao, C. Li, X. Zhang, N. Li, T. Wang, X. Li, C. Wang, G. Qu, X. Xu, *Sci. Bull.* **2023**, *68*, 56–64.
- [41] R. Yao, L. Qian, Y. Sui, G. Zhao, R. Guo, S. Hu, P. Liu, H. Zhu, F. Wang, C. Zhi, C. Yang, *Adv. Energy Mater.* **2022**, *12*, 2102780.
- [42] a) Z. Yang, B. Wang, Y. Chen, W. Zhou, H. Li, R. Zhao, X. Li, T. Zhang, F. Bu, Z. Zhao, W. Li, D. Chao, D. Zhao, *Nat. Sci. Rev.* **2022**, *10*, nwac268; b) W. Zhou, M. Song, P. Liang, X. Li, X. Liu, H. Li, T. Zhang, B. Wang, R. Zhao, Z. Zhao, W. Li, D. Zhao, J. Am. Chem. Soc. **2023**, *145*, 10880–10889.
- [43] Y. Sui, X. Ji, *Chem. Rev.* **2021**, *121*, 6654–6695.
- [44] Y. Zheng, Y. Jiao, Y. Zhu, L. H. Li, Y. Han, Y. Chen, A. Du, M. Jaroniec, S. Z. Qiao, *Nat. Commun.* **2014**, *5*, 3783.
- [45] C.-C. Kao, C. Ye, J. Hao, J. Shan, H. Li, S.-Z. Qiao, *ACS Nano* **2023**, *17*, 3948–3957.
- [46] P. Ruan, X. Chen, L. Qin, Y. Tang, B. Lu, Z. Zeng, S. Liang, J. Zhou, *Adv. Mater.* **2023**, *35*, 2300577.
- [47] A. Chen, C. Zhao, Z. Guo, X. Lu, N. Liu, Y. Zhang, L. Fan, N. Zhang, *Energy Storage Mater.* **2022**, *44*, 353–359.
- [48] X. Liu, F. Yang, W. Xu, Y. Zeng, J. He, X. Lu, *Adv. Sci.* **2020**, *7*, 2002173.
- [49] R. Zhao, J. Yang, X. Han, Y. Wang, Q. Ni, Z. Hu, C. Wu, Y. Bai, *Adv. Energy Mater.* **2023**, *13*, 2203542.
- [50] J. He, Y. Tang, G. Liu, H. Li, M. Ye, Y. Zhang, Q. Yang, X. Liu, C. Li, *Adv. Energy Mater.* **2022**, *12*, 2202661.
- [51] W. Xu, X. Liao, W. Xu, K. Zhao, G. Yao, Q. Wu, *Adv. Mater.* **2023**, *12*, 2300283.
- [52] M. Qiu, P. Sun, Y. Wang, L. Ma, C. Zhi, W. Mai, *Angew. Chem. Int. Ed.* **2022**, *61*, e202210979.
- [53] X. He, Y. Cui, Y. Qian, Y. Wu, H. Ling, H. Zhang, X.-Y. Kong, Y. Zhao, M. Xue, L. Jiang, L. Wen, *J. Am. Chem. Soc.* **2022**, *144*, 11168–11177.
- [54] H. Zhang, Z. Luo, W. Deng, J. Hu, G. Zou, H. Hou, X. Ji, *Chem. Eng. J.* **2023**, *461*, 142105.
- [55] A. Chen, C. Zhao, Z. Guo, X. Lu, J. Zhang, N. Liu, Y. Zhang, N. Zhang, *Energy Storage Mater.* **2022**, *32*, 2203595.
- [56] Z. Shi, S. Chen, Z. Xu, Z. Liu, J. Guo, J. Yin, P. Xu, N. Zhang, W. Zhang, H. N. Alshareef, T. Liu, *Adv. Energy Mater.* **2023**, *13*, 2300331.
- [57] X. Xie, S. Liang, J. Gao, S. Guo, J. Guo, C. Wang, G. Xu, X. Wu, G. Chen, J. Zhou, *Energy Environ. Sci.* **2020**, *13*, 503–510.
- [58] Q. Tan, X. Li, B. Zhang, X. Chen, Y. Tian, H. Wan, L. Zhang, L. Miao, C. Wang, Y. Gan, J. Jiang, Y. Wang, H. Wang, *Adv. Energy Mater.* **2020**, *10*, 2100445.
- [59] T. Wei, Y. Ren, Y. Wang, L. e. Mo, Z. Li, H. Zhang, L. Hu, G. Cao, *ACS Nano* **2023**, *17*, 3765–3775.
- [60] C. Huang, X. Zhao, S. Liu, Y. Hao, Q. Tang, A. Hu, Z. Liu, X. Chen, *Adv. Mater.* **2021**, *33*, 2100445.
- [61] T. Wei, X. Zhang, Y. Ren, Y. Wang, Z. Li, H. Zhang, L. Hu, *Chem. Eng. J.* **2023**, *457*, 141272.
- [62] Y. Zhong, Z. Cheng, H. Zhang, J. Li, D. Liu, Y. Liao, J. Meng, Y. Shen, Y. Huang, *Nano Energy* **2022**, *98*, 107220.
- [63] J. Wan, R. Wang, Z. Liu, L. Zhang, F. Liang, T. Zhou, S. Zhang, L. Zhang, Q. Lu, C. Zhang, Z. Guo, *ACS Nano* **2023**, *17*, 1610–1621.
- [64] L. Zheng, H. Li, X. Wang, Z. Chen, C. Hu, K. Wang, G. Guo, S. Passerini, H. Zhang, *ACS Energy Lett.* **2023**, *8*, 2086–2096.
- [65] K. Wang, F. Liu, Q. Li, J. Zhu, T. Qiu, X.-X. Liu, X. Sun, *Chem. Eng. J.* **2023**, *452*, 139577.
- [66] J. Yang, Y. Zhang, Z. Li, X. Xu, X. Su, J. Lai, Y. Liu, K. Ding, L. Chen, Y.-P. Cai, Q. Zheng, *Adv. Funct. Mater.* **2022**, *32*, 2209642.
- [67] J.-L. Yang, L. Liu, Z. Yu, P. Chen, J. Li, P. A. Dananjaya, E. K. Koh, W. S. Lew, K. Liu, P. Yang, H. J. Fan, *ACS Energy Lett.* **2023**, *8*, 2042–2050.
- [68] J. Yang, R. Zhao, Y. Wang, Z. Hu, Y. Wang, A. Zhang, C. Wu, Y. Bai, *Adv. Funct. Mater.* **2023**, *33*, 2213510.
- [69] H. Yan, S. Li, Y. Nan, S. Yang, B. Li, *Adv. Energy Mater.* **2021**, *11*, 2100186.

Manuscript received: July 8, 2023

Revised manuscript received: August 13, 2023

Accepted manuscript online: August 14, 2023

Version of record online: August 28, 2023